# Models of Factor 430. Structural and Spectroscopic Studies of Ni(II) and Ni(I) Hydroporphyrins

**Mark W. Renner,[1a] Lars R. Furenlid,[1a] Kathleen M. Barkigia,[1a] Arthur Forman,[1a] Hyun-Kwan Shim,[1b] Daniel J. Simpson,[1b] Kevin M. Smith,[1b] and Jack Fajer*[,1a]**

*Contribution from the Department of Applied Science, Brookhaven National Laboratory, Upton, New York 11973, and Department of Chemistry, University of California, Davis, California 95616.* *Received March 8, 1991*

**Abstract:** The reductive chemistry of a series of progressively more saturated Ni(II) porphyrins, derived from anhydromesorhodochlorin XV methyl ester, has been examined as models of F430. Cyclic voltammetry, spectroelectrochemistry, electron paramagnetic resonance, and X-ray absorption studies are used to characterize the parent compounds and their reduction products. Within the Ni(II) porphyrin, chlorin, isobacteriochlorin (iBC), and hexa- and octahydro porphyrin series, only the iBCs are reduced to Ni(I). The other compounds yield $\pi$ anion radicals or $\pi$ radicals with some metal character. The structure of one of the iBCs in the series has been determined by single-crystal X-ray diffraction and used to validate EXAFS results. Crystallographic data for Ni(II) anhydromesorhodoisobacteriochlorin methyl ester with rings C and D reduced, **3**, are the following: space group $P2_1$, $a$ = 13.688 (1) Å, $b$ = 8.124 (1) Å, $c$ = 14.178 (1) Å, $\beta$ = 111.83 (1)°, $V$ = 1463.6 Å$^3$, and $Z$ = 2. The structure was refined against 1226 data points to $R_F$ = 0.058 and $R_{wF}$ = 0.056. Saturation of the macrocycles affects their electronic configurations as evidenced by changes in redox and optical properties as well as sites of reduction. In addition, structural factors emerge as significant determinants of the chemistry of the Ni compounds. Their ability to form Ni(I) or hexacoordinate high-spin Ni(II) requires that the macrocycles be flexible enough to accommodate the conformational changes that accompany reduction to Ni(I) or axial ligation of square-planar Ni(II). Thus, interdependent electronic and structural factors control the reactivity of the models considered here and, by analogy, that of F430 as well.

## Introduction

Methyl coenzyme M reductase catalyzes the final stages of the reduction of carbon dioxide to methane in methanogenic bacteria. The terminal steps involve Factor 430 (F430), a nickel(II) tetrapyrrole whose structure has been deduced by nuclear magnetic resonance to be a hydrocorphin, i.e., a highly saturated porphyrin[2-4] (Figure 1). Detection of EPR signals attributable to Ni(I) in the catalytic cycle of *Methanobacterium thermoautotrophicum*[5] and the observations that isolated Ni(I) F430M (the pentamethyl ester of F430) reacts with methyl iodide and sulfonium salts to yield methane[6,7] have led to intensive investigations of the reductive chemistry of F430[6,7] and nickel porphyrin derivatives.[8-16] Furthermore, the catalytic function of F430 in methane biogenesis has reinforced the long-standing interest in electrochemical and photochemical activation of carbon dioxide by organometallic catalysts for the production of organic fuels.[17-20]

Magnetic circular dichroism[21] and X-ray absorption near-edge[22] studies of F430 in the enzyme complex suggest a hexacoordinate, octahedral Ni(II) environment with two oxygen axial ligands whereas F430 can be isolated in tetra- and hexacoordinate forms.[4d] Extended X-ray absorption (EXAFS) studies have established that the low-spin, square-planar forms of F430 and its 12,13-diepimer are characterized by short Ni-N bonds of 1.9 Å that increase to 2.1 Å upon axial coordination and conversion to a high-spin configuration.[7,22] On the basis of crystallographic studies of Ni corphin and hydroporphyrin models,[4d] the long and short Ni-N distances are diagnostic of planar and ruffled macrocycles, respectively. The F430 skeleton thus exhibits considerable flexibility. Not surprisingly, therefore, the macrocycle can readily accommodate the structural changes, recently observed by EXAFS,[7] that accompany reduction to Ni(I): A distortion occurs

(1) (a) Brookhaven National Laboratory. (b) University of California, Davis.
(2) Fässler, A.; Kobelt, A.; Pfaltz, A.; Eschenmoser, A.; Bladon, C.; Battersby, A. R.; Thauer, R. K. *Helv. Chim. Acta* **1985**, *68*, 2287.
(3) Ellefson, W. L.; Whitman, W. B.; Wolfe, R. S. *Proc. Natl. Acad. Sci. U.S.A.* **1982**, *79*, 3707. Hausinger, R. P.; Orme-Johnson, W. H.; Walsh, C. *Biochemistry* **1984**, *23*, 801. Daniels, L.; Sparling, R.; Sprott, G. D. *Biochim. Biophys. Acta* **1984**, *768*, 113.
(4) For recent reviews, see the following in *The Bioinorganic Chemistry of Nickel*; Lancaster, J. R., Ed.; VCH Publishers: New York, 1988: (a) Eidsness, M. K.; Sullivan, R. J.; Scott, R. A. p 73. (b) Ankel-Fuchs, D.; Thauer, R. K. p 93. (c) Wackett, L. P.; Honek, J. F. Begley, T. P.; Shames, S. L.; Niederhoffer, E. C.; Hausinger, R. P.; Orme-Johnson, W. H.; Walsh, C. T. p 249. (d) Pfaltz, A. p 275.
(5) Albracht, S. P. J.; Ankel-Fuchs, D.; Van der Zwaan, J. W.; Fontijn, R. D.; Thauer, R. K. *Biochim. Biophys. Acta* **1986**, *870*, 50. Albracht, S. P. J.; Ankel-Fuchs, D.; Böcher, R.; Ellerman, J.; Moll, J.; Van der Zwaan, J. W.; Thauer, R. K. *Biochim. Biophys. Acta* **1988**, *955*, 86.
(6) Jaun, B.; Pfaltz, A. *J. Chem. Soc., Chem. Commun.* **1986**, 1327; **1988**, 293.
(7) Furenlid, L. R.; Renner, M. W.; Fajer, J. *J. Am. Chem. Soc.* **1990**, *112*, 8987.
(8) Stolzenberg, A. M.; Stershic, M. T. *Inorg. Chem.* **1987**, *26*, 1970; *J. Am. Chem. Soc.* **1988**, *110*, 5397 and 6391.
(9) Renner, M. W.; Forman, A.; Fajer, J.; Simpson, D.; Smith, K. M.; Barkigia, K. M. *Biophys. J.* **1988**, *53*, 277.
(10) Renner, M. W.; Forman, A.; Wu, W.; Chang, C. K.; Fajer, J. *J. Am. Chem. Soc.* **1989**, *111*, 8618.
(11) Latos-Grazynski, L.; Olmstead, M. M.; Balch, A. L. *Inorg. Chem.* **1989**, *28*, 4066.
(12) Lexa, D.; Momenteau, M.; Mispelter, J.; Saveant, J. M. *Inorg. Chem.* **1989**, *28*, 30.
(13) Kadish, K. M.; Sazou, D.; Maiya, G. B.; Han, B. C.; Liu, Y. M.; Saoiabi, A.; Ferhat, M.; Guilard, R. *Inorg. Chem.* **1989**, *28*, 2542.
(14) Furenlid, L. R.; Renner, M. W.; Smith, K. M.; Fajer, J. *J. Am. Chem. Soc.* **1990**, *112*, 1634.
(15) Nahor, G. S.; Neta, P.; Hambright, P.; Robinson, L. R.; Harriman, A. *J. Phys. Chem.* **1990**, *94*, 6659.
(16) Kadish, K. M.; Franzen, M. M.; Han, B. C.; Araullo-McAdams, C.; Sazou, D. *J. Am. Chem. Soc.* **1991**, *113*, 512.
(17) For recent reviews, see: Creutz, C. In *Electrochemical and Electrocatalytic Reduction of Carbon Dioxide*; Sullivan, B. P., Ed.; Elsevier: Amsterdam, in press. Walther, D. *Coord. Chem. Rev.* **1987**, *79*, 135. Ayers, W. M., Ed. *Catalytic Activation of Carbon Dioxide*; ACS Symposium Series; American Chemical Society: Washington, DC, 1988. Behr, A. *Carbon Dioxide Activation by Metal Complexes*; VCH: Weinheim, 1988. Braunstein, D.; Matt, D.; Nobel, D. *Chem. Rev.* **1988**, *88*, 747. Kolomnikov, I. S.; Lysak, T. V.; Rusakov, S. L.; Kharitonov, Y. Y. *Russ. Chem. Rev.* **1988**, *57*, 406. Behr, A. *Angew. Chem., Int. Engl. Ed.* **1988**, *27*, 661. Collin, J. P.; Sauvage, J. P. *Coord. Chem. Rev.* **1989**, *93*, 245.
(18) Craig, C. A.; Spreer, L. O.; Otvos, J. W.; Calvin, M. *J. Phys. Chem.* **1990**, *94*, 7957.
(19) Espenson, J. H.; Ram, M. S.; Bakac, A. *J. Am. Chem. Soc.* **1987**, *109*, 6892.
(20) Furenlid, L. R.; Renner, M. W.; Szalda, D. J.; Fujita, E. *J. Am. Chem. Soc.* **1991**, *113*, 883.
(21) Cheesman, M. R.; Ankel-Fuchs, D.; Thauer, R. K.; Thompson, A. J. *Biochem. J.* **1989**, *260*, 613. See also: Hamilton, C. L.; Scott, R. A.; Johnson, M. K. *J. Biol. Chem.* **1989**, *264*, 11605.
(22) Shiemke, A. K.; Kaplan, W. A.; Hamilton, C. L.; Shelnutt, J. A.; Scott, R. A. *J. Biol. Chem.* **1989**, *264*, 7276.

0002-7863/91/1513-6891$02.50/0 

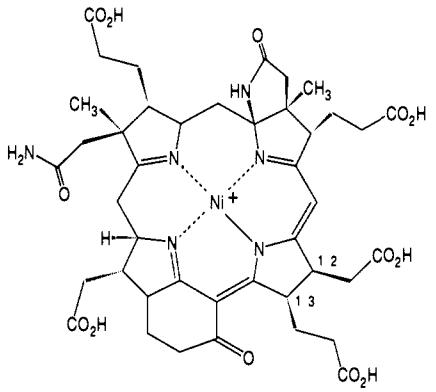

F430

**Figure 1.** Molecular structure of F430.

around the Ni, with two sets of Ni(I)–N distances of 1.88 (±0.03) Å and 2.03 (±0.03) Å. Similar deformations on reduction to Ni(I) have also been observed in isobacteriochlorin[14] and tetraaza[20] complexes whereas formation of Ni(II) $\pi$ anion radicals in chlorins and porphycenes[14] leaves the Ni–N distances unaltered. These results suggest that the ability of the macrocycles to change conformations helps to control the site of reduction (metal vs macrocycle) and, in turn, determines the chemistry of the reduction products. These effects of structural compliance may be part of the more general influence of conformations on the chemical and physical properties of porphyrinic chromophores and prosthetic groups.[23]

In an attempt to delineate the structural and electronic factors that determine the reductive chemistry of F430 and of model porphyrins and hydroporphyrins, we present here redox, optical, EPR, structural, and theoretical results for a homologous series of progressively more saturated Ni(II) porphyrins that incorporate some of the features of F430 (Figure 2).

## Methods

Complexes **3–6** were prepared by Raney nickel reductions of Ni(II) anhydromesorhodochlorin XV methyl ester, **2**, as described by Smith and Simpson.[24] The hexahydroporphyrins **5** and **5′** were isolated as a mixture of two isomers and used without further separation. Porphyrin **1** was obtained by oxidation of **2** with 2,3-dichloro-5,6-dicyanobenzoquinone.[23a] Ni(II) methyl pyropheophorbide *a* **7** was prepared according to Smith and Lai.[25] Ni(II) octaethylporphyrin (OEP), Ni(II) hexakisimidazole chloride,[26] Ni(II) hexamine chloride,[27] and Ni(II) cyclam iodide[28] were used as EXAFS standards. Purities of the hexacoordinate species were verified by elemental analysis. Ni(II) cyclam iodide was obtained in crystalline form by anion exchange with Ni(II) cyclam perchlorate. Ni(II) OEP (Aldrich) was used without further purification.

Tetrahydrofuran (THF) was distilled from Na/benzophenone and stored over Na/K alloy in vacuo. Dichloromethane was distilled from $CaH_2$ and stored over molecular sieves. Piperidine was vacuum distilled from KOH.

Redox potentials were determined by cyclic voltammetry in THF or $CH_2Cl_2$ with 0.1 M $Bu_4NClO_4$ (TBAP) as supporting electrolyte.[29]

One-electron reduction products were generated electrochemically in THF at Pt electrodes in vacuo by using published cell designs and techniques.[30] Optical spectra were recorded at room temperature on Perkin-Elmer 330 or Cary 2300 spectrophotometers. EPR spectra were obtained on a Bruker-IBM ER200D spectrometer equipped with a field frequency lock and an Aspect 2000 data acquisition system. Ni(I) EPR spectra were simulated with a program kindly provided by T. D. Smith and P. Aisen of the Albert Einstein College of Medicine.[31]

X-ray absorption spectra were measured at room temperature at beam line X-11A at the National Synchrotron Light Source. Ni(II) samples were prepared as either fine powders measured in transmission mode, or as ~5 mM THF solutions measured in fluorescence mode in 2-mm-thick teflon cells with thin Mylar windows. The reduced species were measured in recently described anaerobic cells that allow optical and EPR spectra to be verified before and after X-ray exposure.[32]

Data were collected in 8- or 20-min scans, for transmission and fluorescence modes, respectively, yielding a minimum of $10^6$ counts of signal at the Ni K-edge for each sample. Energies were calibrated with a nickel foil via the internal calibration method. Data scans were inspected individually to remove monochromator glitches and insure that no change in signal occurred between the first and last scans.

The EXAFS oscillations for samples and standards were isolated by standard methods:[14,20,33] linear extrapolation and subtraction of a preedge bulk absorption contribution, normalization of the edge step, interpolation onto a photoelectron momentum ($k$) grid, and removal of a smooth background with a series of three or four cubic splines. $E_0$ was defined as the energy corresponding to the midpoint of the main absorption step and $\hbar^2k^2/2m_e = E - E_0$. The resulting oscillations were typically weighted with a $k^3$ factor and Fourier filtered to isolate first-shell contributions as amplitude and phase functions. Quantitative comparisons between unknowns and standards were accomplished with both nonlinear least-squares fitting and ratio methods to deduce the parameters of the EXAFS equation; for details, see ref 20. Errors were estimated by treating data sets individually through the Fourier filter step, and combining the results to give mean ± standard deviation isolated EXAFS, which were then analyzed in the same manner as the averaged data.

$Ni(N_4O_3C_{33}H_{36})$, complex **3**, crystallized from $CHCl_3/CH_3OH$ in monoclinic space group $P2_1$ with $a$ = 13.688 (1) Å, $b$ = 8.124 (1) Å, $c$ = 14.178 (1) Å, $\beta$ = 111.83 (1)°, $V$ = 1463.6 Å$^3$, and $Z$ = 2. Single-crystal diffraction measurements were carried out at room temperature on a crystal of dimensions 0.06 × 0.46 × 0.072 mm$^3$ in the $\theta$ range 2–50°, by using graphite monochromated Cu radiation, $\lambda$ = 1.5418 Å, on an Enraf-Nonius CAD4 diffractometer. A total of 3651 reflections were processed from two quadrants, with $hkl$ and $\bar{h}k\bar{l}$ averaged to give 1641 unique reflections. Data were corrected for Lorentz and polarization effects, and absorption using the analytical method. The structure was solved with MULTAN78 and refined against the 1226 data points having $F_0 > 4\sigma F_0$. Hydrogen atoms were placed in calculated positions, and anisotropic refinement of the Ni and atoms of the side chains using full-matrix least squares yielded $R_F$ = 0.058 and $R_{WF}$ = 0.056, with anomalous contributions to the scattering factors for the Ni atom. The other possible enantiomer was excluded on the basis of higher $R$ values.

**Table I.** Reduction Potentials for Nickel(II) Complexes[a]

| compound | $E_{1/2}$ (V vs SCE) 1 | 2 | solvent |
|---|---|---|---|
| porphyrin **1** | −1.07 | irrev | $CH_2Cl_2$ |
| | −0.99 | −1.35 | THF |
| chlorin **2** | −1.08 | irrev | $CH_2Cl_2$ |
| | −1.04 | −1.42 | THF |
| Pheo **7** | −1.05 | −1.40 | THF |
| iBC **3** | irrev | | $CH_2Cl_2$ |
| | −1.33 | | THF |
| iBC **4** | −1.33 | | THF |
| hexahydroporphyrins **5** and **5′** | −1.45 | | THF |
| octahydroporphyrin **6** | −1.59 | | THF |
| OEP[8] | −1.50 | | $CH_3CN$ |
| OEC[8] | −1.46 | | $CH_3CN$ |
| OEiBC[8] | −1.52 | | $CH_3CN$ |
| F430M[6,7] | irrev | | $CH_2Cl_2$ |
| | −0.95 | | $C_3H_7CN$ |
| F430M diepimer[7] | −1.03 | | $C_3H_7CN$ |

[a] Scan rates 100 mV/s; 0.1 M TBAP electrolyte; room temperature.

(23) (a) Barkigia, K. M.; Berber, M. D.; Fajer, J.; Medforth, C. J.; Renner, M. W.; Smith, K. M. *J. Am. Chem. Soc.* **1990**, *112*, 8851. (b) Renner, M. W.; Cheng, R.-J.; Chang, C. K.; Fajer, J. *J. Phys. Chem.* **1990**, *94*, 8508 and references therein.
(24) Smith, K. M.; Simpson, D. J. *J. Am. Chem. Soc.* **1987**, *109*, 6326.
(25) Smith, K. M.; Lai, J. J. *J. Am. Chem. Soc.* **1984**, *106*, 5746.
(26) Konopelski, J. P.; Reimann, C. W.; Hubbard, C. R.; Mighell, A. D.; Santoro, A. *Acta Crystallogr.* **1976**, *B32*, 2911.
(27) Furenlid, L. R. Ph.D. Dissertation, Georgia Institute of Technology, 1988. Wyckoff, R. W. G. *Crystal Structures*; Interscience: New York, 1965; p 783.
(28) Prasad, L.; McAuley, A. *Acta Crystallogr.* **1983**, *C39*, 1175.
(29) Fujita, I.; Chang, C. K. *J. Chem. Educ.* **1984**, *61*, 913.
(30) Fajer, J.; Fujita, I.; Davis, M. S.; Forman, A.; Hanson, L. K.; Smith, K. M. *Adv. Chem. Ser.* **1982**, *201*, 489.
(31) Toy, A. D.; Chaston, S. H. H.; Pilbrow, J. R.; Smith, T. D. *Inorg. Chem.* **1971**, *10*, 2219.
(32) Furenlid, L. R.; Renner, M. W.; Fajer, J. *Rev. Sci. Instrum.* **1990**, *61*, 1326.
(33) Stern, E. A.; Heald, S. M. *Handbook on Synchrotron Radiation*; Koch, E. E., Ed.; North Holland: Amsterdam, 1983; Vol. 1; see also references therein.

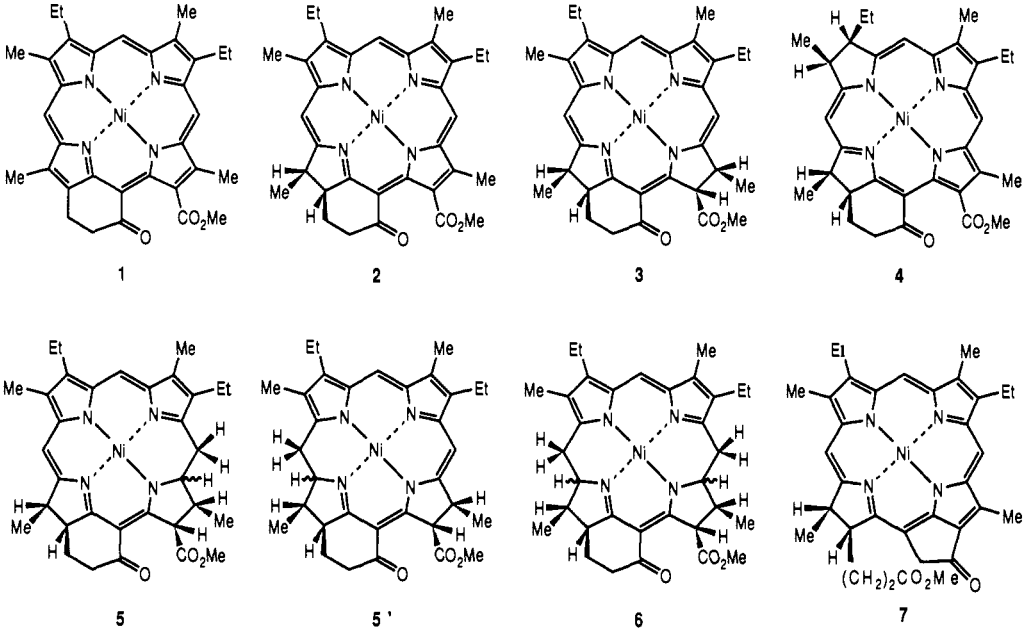


**Figure 2.** Structures of the Ni(II) porphyrin **1**, chlorin **2**, isobacteriochlorin (CD) **3**, isobacteriochlorin (AD) **4**, hexahydroporphyrins **5** and **5'**, octahydroporphyrin **6**, and methyl pyropheophorbide *a* **7**.

**Table II.** Oxidation Potentials for Ni(II) Complexes[a]

| compound | $E_{1/2}$ (V vs SCE) |
|---|---|
| porphyrin **1** | 0.98 |
| chlorin **2** | 0.77 |
| Pheo **7** | 0.76 |
| iBC **3** | 0.43 |
| hexahydroporphyrins **5** and **5'** | 0.35 |
| octahydroporphyrin **6** | 0.64 |
| OEP[37] | 0.77 |
| OEC[37] | 0.48 |
| OEiBC[37] | 0.21 |
| F430M[42] | 1.28[b] |

[a] In $CH_2Cl_2$ at room temperature; 0.1 M TBAP electrolyte; scan rates 100 mV/s. [b] In $CH_3CN$ with 0.1 M $Bu_4NBF_4$. Reported[42] as 0.825 vs $Fc/Fc^+$.

The iterative extended Hückel (IEH) programs used for MO calculations are described in ref 34. Parameters were taken from Gouterman and Zerner.[35] The coordinates used are discussed in the text. INDO/s computations utilized programs developed by Zerner and co-workers for calculating the optical spectra of closed- and open-shell porphyrins.[36]

## Results and Discussion

**Electrochemistry.** Half-wave redox potentials for the series **1–6**, obtained by cyclic voltammetry, are listed in Tables I and II. Previously reported data for the series of octaethylporphyrin, chlorin, and isobacteriochlorin[8] (OEP, OEC, and OEiBC) as well as for F430M[6,7] are included for comparison. In non-halogenated solvents, all the compounds undergo reversible one-electron reductions. **1** and **2** exhibit approximately the same midpoint potentials whereas **3–6** become harder to reduce as the macrocycles are progressively saturated. The porphyrin **1** and chlorin **2** also display a second reversible one-electron reduction. Note that **1–4** are considerably easier to reduce than the comparable octaethyl series. We attribute this effect to the coupling of the electronegative keto group of the cyclohexanone ring to the macrocycle $\pi$ systems. Indeed, a similar effect is observed for Ni(II) methyl pyropheophorbide (Pheo, **7**), which incorporates a five-membered exocyclic ring with a similar keto function. Analogous effects of electron-withdrawing groups on the redox properties of porphyrins have been noted.[37] Although F430M and its diepimer are considerably more saturated than compounds **1–7**, their reduction potentials[6,7] are close to those of the porphyrin and chlorin. Besides the contribution of the cyclohexanone ring, the compounds are isolated as positively charged complexes,[6] which should make them more electrophilic. In contrast to the reversible behavior of the above compounds in THF, acetonitrile,[8] butyronitrile,[7] or dimethylformamide,[6] the reductions of the iBC, hexahydro, and octahydro porphyrins are irreversible in $CH_2Cl_2$, as are the second reductions of the porphyrin and chlorin. Similar irreversibilities were previously noted for F430[6] and NiOEiBC.[8] Both compounds were shown to react catalytically with methyl iodide to yield methane.[6,8] The two iBC isomers studied here (**3** and **4**) also show electrocatalytic reductions in the presence of $CH_3I$: A large increase in the cyclic voltammetric reduction wave is observed with the disappearance of the reverse wave, behavior characteristic of a diffusion-controlled catalytic process.[38] (Figure 3)

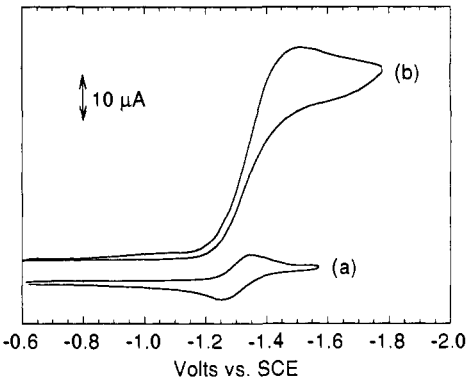


**Figure 3.** Cyclic voltammograms of Ni(II) iBC **3** without (a) and with methyl iodide (b) (20:1, $CH_3I$/iBC) in THF, 0.1 M TBAP, volts vs SCE, scan rate 100 mV/s, at room temperature.

The optical and EPR data that characterize the nature of the products obtained on electroreduction are presented in the next section.

Although the thrust of this work is the reductive chemistry of Ni hydroporphyrins, it is instructive to compare the oxidations of the above series with previously reported results for the octaethyl

(34) Davis, M. S.; Forman, A.; Hanson, L. K.; Thornber, J. P.; Fajer, J. *J. Phys. Chem.* **1979**, *83*, 3325. Chang, C. K.; Hanson, L. K.; Richardson, P. F.; Young, R.; Fajer, J. *Proc. Natl. Acad. Sci. U.S.A.* **1981**, *78*, 2652.
(35) Zerner, M.; Gouterman, M. *Theor. Chim. Acta* **1964**, *4*, 44.
(36) Edwards, W. D.; Zerner, M. C. *Can. J. Chem.* **1985**, *63*, 1763. Thompson, M. A.; Zerner, M. C.; Fajer, J. *J. Phys. Chem.* **1990**, *94*, 3820.
(37) Kadish, K. M. In *Progress in Inorganic Chemistry*; Lippard, S. J., Ed.; Wiley & Sons: New York, 1986; Vol. 34, p 435.
(38) Bard, A. J.; Faulkner, L. R. *Electrochemical Methods*, J. Wiley & Sons: New York, 1980; pp 431, 455.

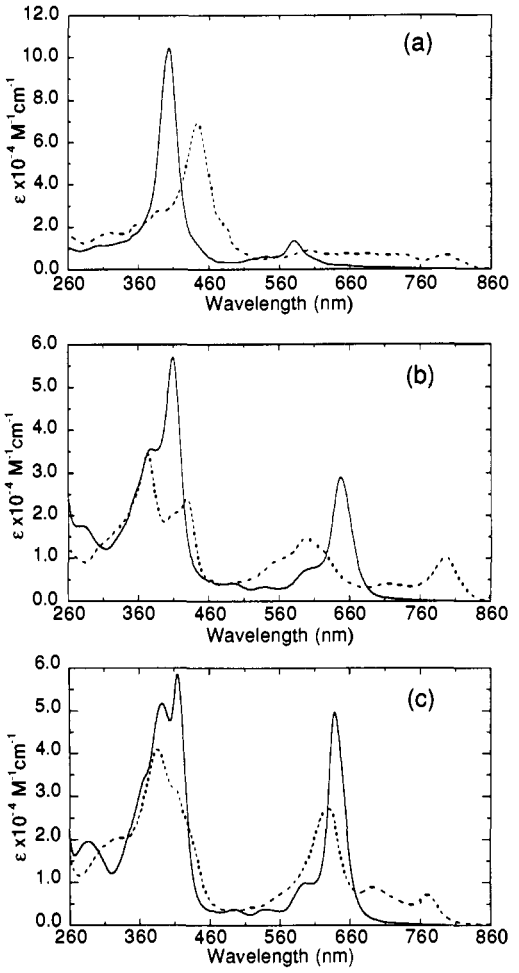


**Figure 4.** Optical spectra of the Ni(II) compounds (—) and their one-electron reduction products (---) in THF at room temperature: (a) porphyrin **1**, (b) chlorin **2**, and (c) pheophorbide **7**. The counterion is $Bu_4N^+$ for the anions.

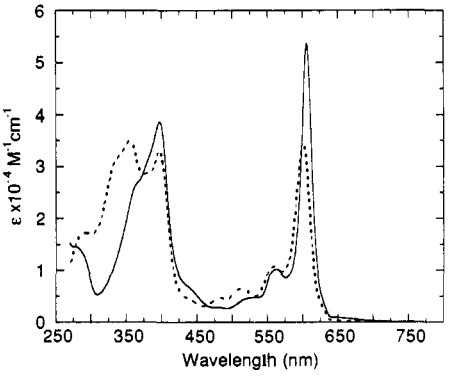


**Figure 5.** Optical spectra of Ni(II) (—) and Ni(I) (---) iBC **3** in THF at room temperature.

derivatives and F430M (Table II). Compounds **1–3** and **5** become progressively easier to oxidize upon increased saturation, as do the octaethyl derivatives. Stolzenberg and Stershic have shown the latter to be oxidized to Ni(II) $\pi$ cations.[39] The trend in ease of oxidation parallels that observed in Zn, free base, and iron porphyrins and hydroporphyrins.[34,40,41] The exocyclic rings with keto functions again influence the redox potentials, but the

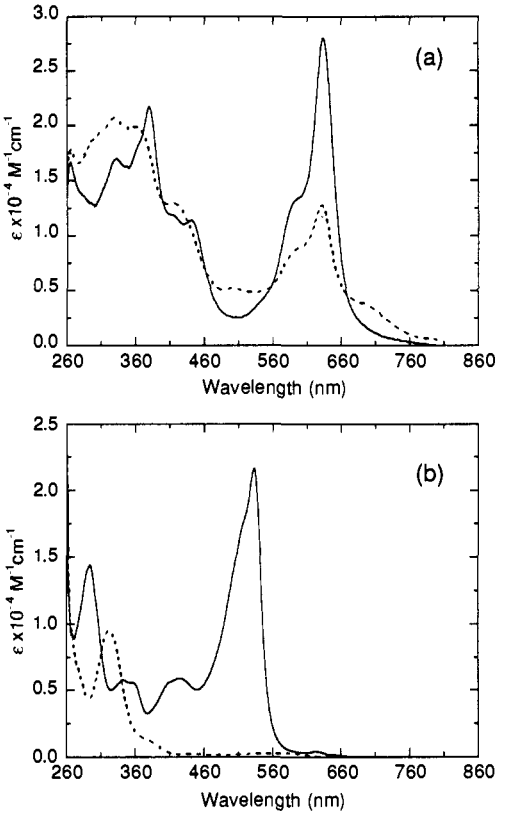


**Figure 6.** Optical spectra of the Ni(II) derivatives (—) and their one-electron reduction products (---) in THF at room temperature: (a) hexahydroporphyrins **5** and **5'** and (b) octahydroporphyrin **6**.

electronegative groups now render the macrocycles harder to oxidize. Saturation to the octahydroporphyrin **6** level reverses the oxidative trend observed in **1–5**, and **6** becomes harder to oxidize. F430M itself is still harder to oxidize ($E_{1/2}$ = 1.28 V), again a consequence of its cationic character, and yields a Ni(III) species.[42]

**Spectroelectrochemistry. (a) Optical Spectra.** Optical spectra for the Ni(II) parent compounds and their one-electron reduction products are shown in Figures 4–6. All the reductions required 1 (±0.05) electron to generate the spectra shown. One-electron reoxidations regenerated >95% of the original spectra.

The spectra of reduced **1**, **2**, and **7** (Figure 4) are typical of $\pi$ anion radicals: The low-energy absorption bands of the parents diminish in intensity and are replaced by weaker, broad bands that extend into the near infrared.[43] The close similarity between the spectra of the two chlorins **2** and **7** is particularly noteworthy. Because of their function in the primary photosynthetic charge separation of green plants, the optical, EPR, and ENDOR properties of reduced chlorophyll and pheophytin *a* have been studied extensively and have unambiguously established the $\pi$ radical nature of the anions. The anion of **7** exhibits optical features almost identical with those of the $\pi$ radicals of the two photosynthetic chromophores.[30,44]

In contrast to the above results, reduction of the isobacteriochlorin **3** causes only a small blue shift of the first absorption band (≈6 nm) and no new red bands appear (Figure 5). Similar spectral changes were reported on reduction of NiOEiBC[8] and are generally diagnostic of metal-centered reductions.[43]

The spectral changes that reflect the reduction of the more saturated hexahydro- and octahydroporphyrins **5** and **6** are shown in Figure 6. No previous data exist to guide assignments of reduction sites; however, the changes observed in the low-energy region imply perturbations of the $\pi$ systems of the molecules.

(39) Stolzenberg, A. M.; Stershic, M. T. *Inorg. Chem.* **1988**, *27*, 1614.
(40) Stolzenberg, A. M.; Spreer, L. O.; Holm, R. H. *J. Am. Chem. Soc.* **1980**, *102*, 364. Stolzenberg, A. M.; Strauss, S. H.; Holm, R. H. *J. Am. Chem. Soc.* **1981**, *103*, 4763.
(41) Richardson, P. F.; Chang, C. K.; Hanson, L. K.; Spaulding, L. D.; Fajer, J. *J. Phys. Chem.* **1979**, *83*, 3420. Richardson, P. F.; Chang, C. K.; Spaulding, L. D.; Fajer, J. *J. Am. Chem. Soc.* **1979**, *101*, 7736. Chang, C. K.; Fajer, J. *J. Am. Chem. Soc.* **1980**, *102*, 848.
(42) Jaun, B. *Helv. Chim. Acta* **1990**, *73*, 2209.
(43) Felton, R. H. In *The Porphyrins*; Dolphin, D., Ed.; Academic Press: New York, 1978; Vol. 5, p 53.
(44) Fujita, I.; Davis, M. S.; Fajer, J. *J. Am. Chem. Soc.* **1981**, *100*, 6280.

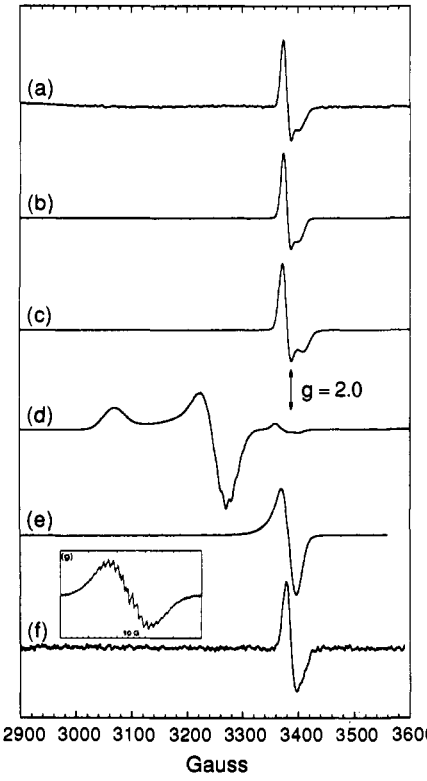


**Figure 7.** EPR spectra of the Ni(II) anion radicals in THF at 113 K: (a) porphyrin **1**, (b) chlorin **2**, (c) Pheo **7**, (e) hexahydroporphyrins **5** and **5'**, and (f) octahydroporphyrin **6**. The inset (g) shows the room-temperature spectrum of the latter ($g$ value = 2.0029). (d) is the spectrum of the Ni(I) iBC **3**.

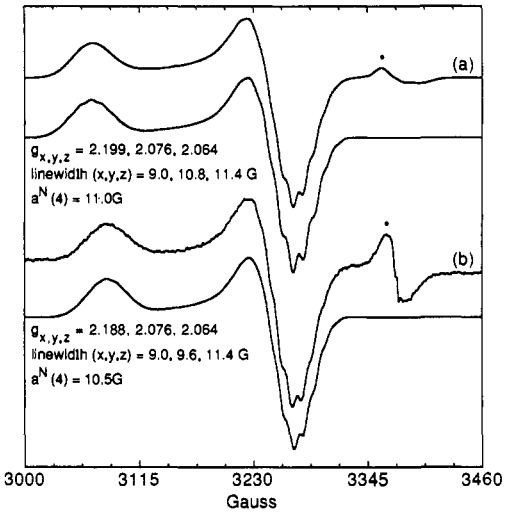


**Figure 8.** EPR spectra and simulations of the Ni(I) iBCs **3** (a) and **4** (b) in THF at 113 K. The peaks marked with an asterisk are free radical impurities that represent less than 5% of the total signals.

More definite assignments can be made for all the compounds considered here, on the basis of EPR results.

**(b) EPR Spectra.** EPR results for the reduced nickel compounds **1–7** in THF at 113 K are shown in Figures 7 and 8.

The isobacteriochlorin spectra are readily assigned to Ni(I) species with an electron added to the $d_{x^2-y^2}$ orbital of the Ni. Simulations yield $g$ values of 2.199, 2.076, and 2.064 with average nitrogen hyperfine splittings[45] of 11 G for isomer **3**, and $g$ = 2.188, 2.076, and 2.064 with $a_N$ = 10.5 G for isomer **4**, (Figure 8). These

(45) Reasonable simulations of the experimental spectra can be obtained with two sets of two nitrogens whose coupling constants differ by 10%.

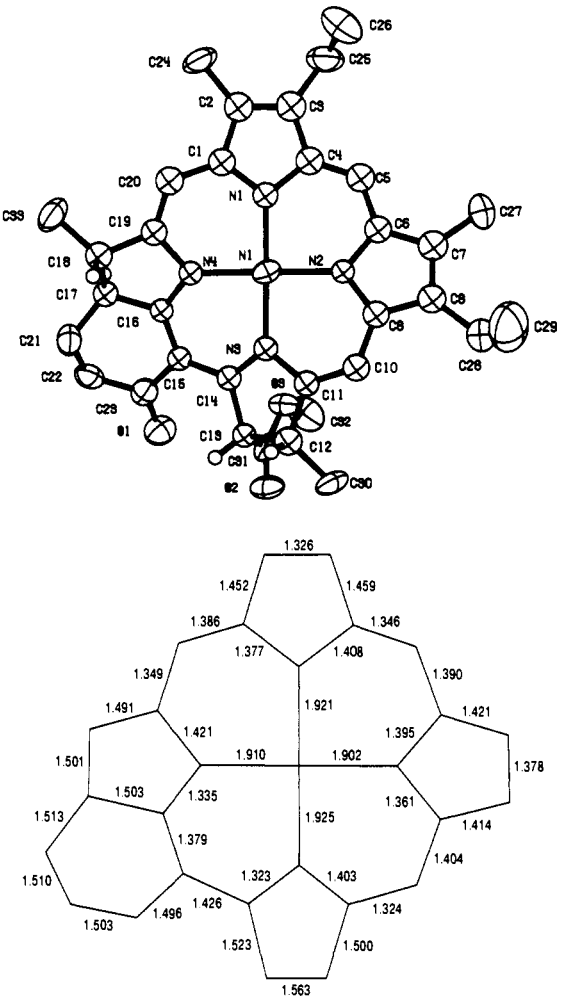





**Figure 9.** Atom names and molecular structure of **3** (top) and bond distances (bottom). The esd's are 0.012 Å for a typical C–C bond and 0.007 Å for the Ni–N distances.

values are similar to those found for Ni(I) complexes of OEiBC,[8] tetraaza derivatives,[46] thiaporphyrins,[47] and F430M.[6,7] For the latter, $g$ = 2.250, 2.074, and 2.065 with $a_N$ = 9.5 G.[6,7]

The hexahydro and octahydro compounds **5** and **6** exhibit narrow signals centered at $g$ = 2.005 characteristic of $\pi$ radicals (Figure 7). In addition, **6** displays hyperfine structure at room temperature (inset, Figure 7) that further reinforces the assignment of a $\pi$ radical.

Porphyrin **1** and chlorins **2** and **7** also yield $g$ = 2 signals, but the spectra are anisotropic with a high-field shoulder at $g$ = 1.99 suggesting some metal character to the $\pi$ radical. The EPR signals could not be saturated, further supporting interactions between the metal and the free radicals. Similar anisotropic spectra have been noted for other Ni(II) porphyrin $\pi$ anions[16] and for Fe(II) iBC $\pi$ cations.[48]

The above spectral results establish that, within the series **1–7**, only the isobacteriochlorins are reduced to Ni(I) whereas the other compounds yield $\pi$ anions. The question arises as to why the compounds at higher saturation levels than iBC are reduced to radicals rather than to Ni(I). We have suggested above the possibility that structural as well as electronic factors may control redox sites. We present next the results for both crystallographic and X-ray absorption experiments which support that premise.

(46) Lovecchio, F. V.; Gore, E. S.; Busch, D. H. *J. Am. Chem. Soc.* **1974**, *96*, 3109.
(47) Chmielewski, P.; Grzeszczuk, M.; Latos-Grazynski, L.; Lisowski, J. *Inorg. Chem.* **1989**, *28*, 3546.
(48) Sullivan, E. P.; Strauss, S. H. *Inorg. Chem.* **1989**, *28*, 3093.

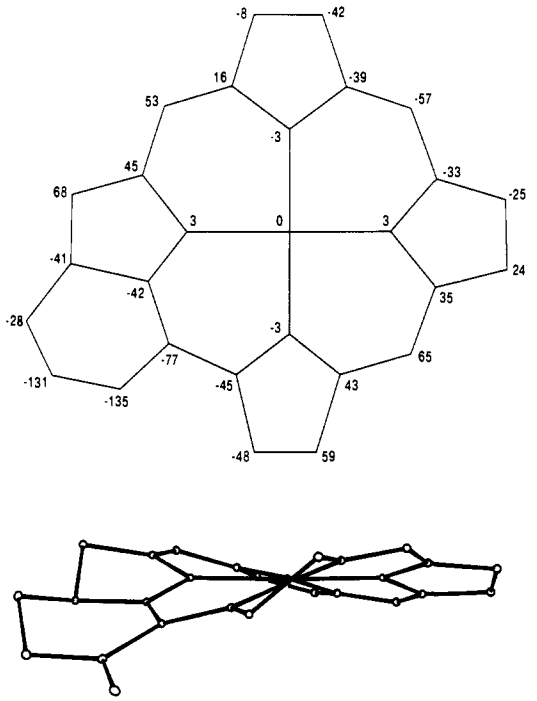


**Figure 10.** Deviations in units of 0.01 Å from the plane defined by the four nitrogens in **3** (top) and an edge-on view of the skeleton of **3** that illustrates its conformational ruffling (bottom).

**Structural Results. (a) Crystal Structure of the Ni(II) Isobacteriochlorin 3.** The crystal structure of **3** was undertaken to determine the conformation of the macrocycle and to assess the possible structural effects of the exocyclic cyclohexanone, also present in F430. One high-precision structure within the anhydro series would serve to validate X-ray absorption results and provide a basis for electronic structure calculations. The molecular structure and atom names of **3** are shown in Figure 9, as are bond distances for its skeleton. The molecules form stacks with the closest approach between ring D centers of 4.4 Å and Ni–Ni distances of 6.25 Å.

The saturated rings in the molecule exhibit the expected features:[49-51] elongated Cα–Cβ and Cβ–Cβ bonds and broader Cα–N–Cα angles, with average values[52] of 1.504 (7) Å, 1.532 (13) Å, and 107.1 (7)°, respectively. The exocyclic ring adopts a half-chair conformation in which the C–C distances are typical of single bonds, and the C=O length of 1.233 (10) Å is comparable to those found in chlorophyll exocyclic rings, 1.222 (4) Å in methyl bacteriopheophorbide *a*, for example.[51] The results establish that the hydrogens in ring C are in a cis configuration.

The Ni lies in the plane of the four nitrogens, and the Ni–N distances of 1.902, 1.910, 1.921, and 1.925 Å average to 1.915 (5) Å. They are typical of the short Ni–N distances found in ruffled, low-spin Ni hydroporphyrins.[49,50b] The severe $S_4$ ruffling pattern of **3** is evident in the edge-on view and the deviations from the plane of the four nitrogens presented in Figure 10. The angles between the planes of adjacent rings average 34°, and the mean dihedral angle around the Cβ–Cβ bonds of the saturated rings is 29.6°. The fused exocyclic ring appears to have little influence on the conformation of the macrocycle. Comparison of the bond angles, distances, and deviations from the mean plane of **3** with those in the structure of Ni(II) 5,10,15,20-tetramethylisobacteriochlorin[50b] shows only minor differences. The average Cβ–Cβ bonds in the pyrroline rings in **3** are slightly longer (+0.035 Å) than in the tetramethyl derivative, consistent with their bulkier substituents. The Ni–N distances to both the saturated and unsaturated rings agree within 0.004 and 0.008 Å, respectively. Thus, there are no major structural consequences associated with incorporation of the exocyclic ring evident in the $S_4$ ruffled conformation of the isobacteriochlorin. Additional details of the structure can be found in the supplementary material, which includes positional and thermal parameters and structure factors.

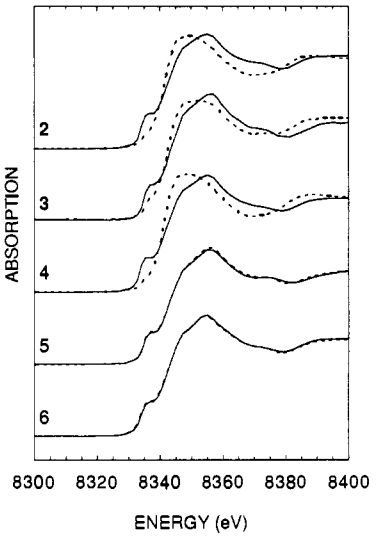


**Figure 11.** X-ray absorption near-edge spectra of the Ni(II) compounds **2**–**6** before (—) and after (---) addition of piperidine (in THF at room temperature).

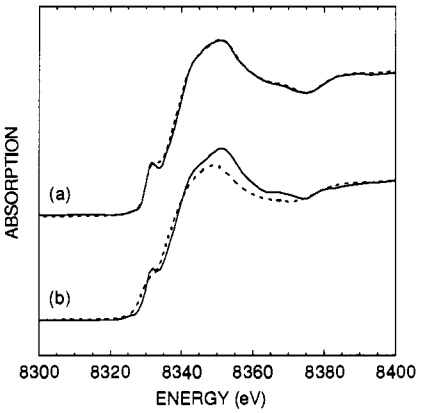


**Figure 12.** X-ray absorption edge spectra of (a) the Ni(II) chlorin **2** (—) and its π radical (---) and (b) the Ni(II) iBC **3** (—) and its Ni(I) anion (---) (in THF at room temperature).

**(b) X-ray Near-Edge Structure.** The X-ray absorption edges of nickel complexes have been shown to be highly sensitive to the coordination geometry around the metal.[4a,22,53] In square-planar complexes, a distinct peak, attributed to a 1s → $4p_z$ electronic transition, is present at approximately 6 eV below the main absorption edge. Introduction of one axial ligand results in attenuation of this peak together with the enhancement of a weakly allowed 1s → 3d peak, arising from the reduction in symmetry. Addition of a second ligand to form octahedral Ni results in the disappearance of the preedge peaks. Edge studies thus serve as convenient probes of the coordination geometry of the Ni complexes. In addition, the edge positions are sensitive to the oxidation state of the Ni[4a,7,20] and hence provide an independent method to verify the assignments of Ni(I) and Ni(II) π radicals reached

(49) Eschenmoser, A. *Ann. N.Y. Sci.* **1986**, *471*, 108. Kratky, C.; Waditschatka, R.; Angst, C.; Johansen, J. E.; Plaquevent, J. C.; Schreiberg, J.; Eschenmoser, A. *Helv. Chim. Acta* **1985**, *68*, 1312 and references therein.

(50) (a) Strauss, S. H.; Silver, M. E.; Long, K. M.; Thompson, R. G.; Hudgens, R. A.; Spartalian, K.; Ibers, J. A. *J. Am. Chem. Soc.* **1985**, *107*, 4207. (b) Suh, M. P.; Swepston, P. N.; Ibers, J. A. *J. Am. Chem. Soc.* **1984**, *106*, 5164.

(51) Barkigia, K. M.; Goufried, D. S.; Boxer, S. G.; Fajer, J. *J. Am. Chem. Soc.* **1989**, *111*, 6444.

(52) The estimated standard deviation of the mean was calculated as $[\sum_m (l_m - \bar{l})^2/m(m-1)]^{1/2}$ for more than two contributors and as the average of the esd's for two contributors.

(53) Eidsness, M. K.; Sullivan, R. J.; Schwartz, J. R.; Hartzell, P. L.; Wolfe, R. S.; Flank, A.-M.; Cramer, S. P.; Scott, R. A. *J. Am. Chem. Soc.* **1986**, *108*, 3120.

**Table III.** Summary of EXAFS Results[a]

| complex | $N$ | $R$ (Å) | $\Delta\sigma^2$ ($\alpha^2 \pm 0.001$) | $\chi^2$(gof) |
|---|---|---|---|---|
| Ni porphyrin **1** | 3.7 ± 0.4 | 1.96 ± 0.02 | 0.0002 | 0.0035 |
| Ni chlorin **2** | 4.0 ± 0.4 | 1.95 ± 0.02 | 0.0003 | 0.0024 |
| Ni iBC (CD) **3** | 3.7 ± 0.4 | 1.93 ± 0.02 | 0.0003 | 0.0019 |
| Ni iBC (AD) **4** | 3.9 ± 0.4 | 1.94 ± 0.02 | −0.001 | 0.034 |
| Ni hexahydro **5** and **5″** | 3.9 ± 0.4 | 1.92 ± 0.02 | 0.0007 | 0.0018 |
| Ni octahydro **6** | 4.0 ± 0.4 | 1.93 ± 0.02 | 0.0002 | 0.016 |
| Ni chlorin **2** + | 4.5 | 2.05 ± 0.02 | 0.004 | 0.037 |
| piperidine | 1.5 (±0.6) | 2.25 ± 0.05 | 0.006 | |
| Ni(I) iBC **3**[14] | 2 | 1.85 ± 0.05 | −0.002 | |
| | 2 | 2.00 ± 0.03 | −0.002 | |
| Ni(II)F430M[7] | 4.3 ± 0.4 | 1.90 ± 0.02 | 0.002 | |
| Ni(I)F430M[7] | 2 | 1.88 ± 0.03 | −0.002 | |
| | 2 | 2.03 ± 0.02 | −0.002 | |
| Ni(II)F430[22] | 6 | 2.10 | 0.003 | |
| Ni(II)F430[22] 12,13-diepimer | 4 | 1.89 | 0.0001 | |

[a] Fourier filter parameters: $k$ range, 3.5–13.5 Å$^{-1}$; Hanning window width, 0.5 Å$^{-1}$; weighting, $k^3$; $R$ range, 1.05–1.95 Å; Hanning window width, 0.1 Å. Fitting range, 4–13 Å$^{-1}$. Standards: NiOEP, $Ni(ImH)_6Cl_2$, NiCyclam $I_2$. $\chi^2$(gof) = $\Sigma$(experiment − fit)$^2$/$\Sigma$experiment$^2$.

on the basis of the optical and EPR results.

The X-ray absorption edge spectra of compounds **2–6** in THF are shown in Figure 11, before and after addition of piperidine. The initial spectra all exhibit the peak diagnostic of square-planar Ni(II) configurations. Upon addition of the ligand, that characteristic feature is lost in the chlorin and the isobacteriochlorins, indicating conversion to hexacoordinated Ni, whereas the hexahydro and octahydro spectra remain unchanged, even at 5 M piperidine. Thus, the latter compounds do not easily accommodate axial ligands.

As shown in Figure 12, the absorption edges of two representative reduced samples are clearly different when the metal or the macrocycle is reduced. The Ni(II) anion radical of the chlorin **2** exhibits edge features virtually identical with its unreduced form. In contrast, the edge of the Ni(I) isobacteriochlorin **3** is visibly different from its neutral parent, with an edge shift of ~3 eV. The preedge feature stays prominent, nonetheless, suggesting that the Ni(I) remains in a planar tetracoordinate environment and does not tightly bind a counterion as a fifth ligand. Obviously, the same conclusions apply to the Ni(II) anion radical. Similar results were previously found for Ni(II) and Ni(I) F430M,[7] and tetraaza complexes.[20]

**(c) Extended X-ray Absorption Fine Structure.** EXAFS results were obtained for the Ni(II) model compounds to assess the structural consequences of the progressive saturation of the macrocycles. Comparison with the crystallographic results for **3** presented above validates the EXAFS results and helps to establish whether the structure of the compound differs in the solid and in solution. The results presented in Table III show that the Ni(II)–N distances in the solid agree within 0.02 Å with the crystallographic results for **3**. No significant differences were found between the solid and its THF solution. (Figures of raw EXAFS data, isolated first-shell contributions, and computed fits have been deposited as supplementary material.)

The series of Ni(II) model complexes shows a trend toward short Ni–N bond lengths with increasing saturation, although the distances fall within a narrow range and lie marginally within the error bars[54] (Table III and Figure 13). As evidenced by the crystallographic results for **3** shown above, and for an extensive series of low-spin Ni(II) hydroporphyrins,[4d,49,50] the short Ni–N distances reflect significantly ruffled macrocycles. Axial ligation of the metal results in an octahedral environment with longer equatorial Ni–N distances and planar macrocycle conformations.[4] Indeed, analysis of the EXAFS spectra of the hexacoordinated Ni(II) chlorin **2** in the presence of piperidine (see edge studies, above) yields *two* sets of Ni–N distances of 2.05 and 2.25 Å

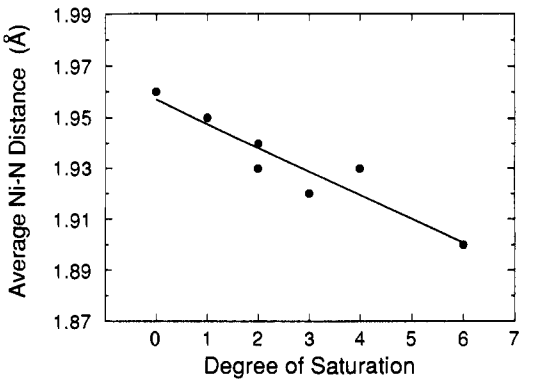


**Figure 13.** Low-spin Ni(II)–N distances plotted as a function of the degree of saturation of the macrocycles with porphyrin = 0, chlorin = 1, iBC = 2, hexahydroporphyrin = 3, octahydroporphyrin = 4, and F430 = 6. Data are taken from Table III. Error estimates are 0.01–0.02 Å.

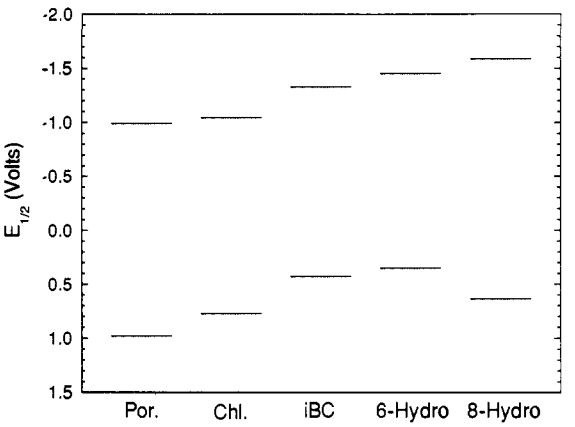


**Figure 14.** Experimental trends in redox potentials plotted as a function of the degree of saturation of the macrocycles. Oxidation potentials were obtained in $CH_2Cl_2$, reduction potentials in THF. Junction potential differences in the two solvents are ~50 mV and are neglected.

assigned to the equatorial porphyrin and axial piperidine Ni–N bonds, respectively. Similar changes in the Ni–N distances have been noted for F430M and its diepimer,[7,22] and thus illustrate the considerable flexibility of the macrocycles.

As reported earlier, the reduced Ni(I) iBC anion **3** shows a significant splitting of the first shell into two long (2.00 ± 0.03 Å) and two short (1.85 ± 0.05 Å) Ni–N bonds.[14] Two distinct metal–nitrogen distances have been observed for every in-plane Ni(I) complex examined so far, including F430M,[7] its 12,13-diepimer,[55] OEiBC,[55] as well as *cis*- and *trans*-tetraazadienes.[20,56] In contrast, the geometry of the Ni chlorin **2** remained virtually *unchanged* on reduction to a $\pi$ anion radical. The unfiltered EXAFS spectra were superimposable, indicating that the structural similarities extend beyond the first shell.[14]

**Electronic Considerations.** The experimental redox potentials for the anhydro series are plotted in Figure 14. The redox potentials reflect the energy levels of the highest occupied (HOMO) and lowest unoccupied (LUMO) molecular orbitals of the complexes, and the differences between oxidation and reduction potentials provide an indication of the energy of the first absorption band of porphyrins and hydroporphyrins[43] since this transition is principally a HOMO to LUMO excitation[34] (with the obvious exception of the iBC complexes where the reduction potentials represent the reduction of Ni(II) to Ni(I)).

Summation of the potentials listed in Tables I and II yields values of 1.97, 1.81, (1.76), 1.80, and 2.29 V for **1**, **2**, **3**, **5**, and **6** respectively, to be compared to the energies of the first optical

(54) The uncertainty of ±0.02 Å reflects an estimate of the error based on comparison with crystallographic results. The differences in Ni–N distances within the homologous series considered here are expected to be closer to ±0.01 Å.

(55) Unpublished results.

(56) The distortions about the Ni(I) and the in-plane position of the atom, deduced by EXAFS analysis, were confirmed by a single crystal structure of (5,7,7,12,12-hexamethyl-1,4,8,11-tetraazacyclotetradeca-4,11-diene)nickel(I) perchlorate.[20]

absorption bands of 2.13, 1.91, (2.04), 1.95, and 2.33 eV, respectively (1240 nm = 1 eV). To a first approximation, the energies of the optical transitions follow the differences in redox potentials (again with the worst deviation for the Ni iBC), and thus lend support to the notion that the potentials reflect the relative energies of the HOMOs and LUMOs of the macrocycles, and that the assignments of $\pi$ anions for **1**, **2**, **5**, and **6** are correct.

Previous experimental results for Zn and free base porphyrins, chlorins, and isobacteriochlorins have established the reduction potential trend as P ≈ Chl with iBC hardest to reduce. Oxidations become concomitantly easier with increased saturation.[34,40,41] Extended Hückel calculations correctly predicted the redox trends and the energy gaps between HOMOs and LUMOs.[34] Theoretical attempts to treat the present Ni series have been less successful. Particularly, the calculated energy gaps between the HOMOs and LUMOs for the hexahydro and octahydro derivatives are too small, and the relative ordering of the Ni and $\pi^*$ orbitals in the iBC is incorrect. (The calculated energy level diagram is included in the supplementary material). Reasons for the discrepancies probably arise from the fact that the structures of the more saturated compounds are not known and that the distortion[14] due to the reduction of Ni(II) to Ni(I) propagates throughout the iBC skeleton. Nonetheless, the extended Hückel calculations do predict the general redox trends observed experimentally. Within the Ni series, the HOMOs rise with saturation; i.e., the molecules become easier to oxidize, as observed. The LUMOs for the porphyrin and chlorin have similar energies, the iBC and hexahydro derivatives are harder to reduce, and the octahydro complex still harder, again in general agreement with the experimental reduction potentials. As noted above, the ordering of the Ni and $\pi$ orbitals in the iBC is not correct but the gap between them does decrease compared to the porphyrin or chlorin.

The energy of the Ni $d_{x^2-y^2}$ orbital appears to be very sensitive to the Ni–N distances. Starting with the planar triclinic NiOEP structure,[57] the $d_{x^2-y^2}$ orbital energies remain roughly constant in the series if the Ni–N distances are held constant, decrease if the core is expanded, and rise if the latter is contracted. Calculations that use the ruffled structures of **3** or Ni tetramethyl iBC[50b] follow similar patterns: Increasing the Ni–N distances shifts the metal orbitals to lower energies, closer to the $\pi^*$ macrocycle levels. Increasing the Ni–N distances to the experimental high-spin values of 2.1 Å causes the $d_{x^2-y^2}$ orbital to drop below the $\pi^*$ orbital.

INDO/s calculations,[36] based on the structure of **3**, predict that formation of Ni(I) iBC should cause only a small blue shift of ~30 nm in the first absorption, in accord with the experimental trend. Similar calculations of Ni(II) porphinoid $\pi$ anions also correctly predict the spectral features of the radicals.[10]

Consideration of the energy levels indicated by the reduction potentials may offer some insights into the chemistry observed. The EPR data for the porphyrin **1** and the chlorin **2** indicate some interaction between the $\pi$ anions and the metal. The Ni orbitals must therefore lie reasonably close to the $\pi^*$ levels. In iBC, the Ni orbital clearly lies below the $\pi^*$ orbitals since Ni(I) is formed upon reduction. The question then arises as to why the hexahydro and octahydro compounds, which are harder to reduce than the iBC, do not yield Ni(I) species. The answer may simply be that saturation at the meso positions renders the macrocycles too rigid to accommodate the structural distortions, observed by EXAFS,[7,14,20] that accompany Ni(I) formation. (Recall that formation of a $\pi$ anion radical causes no significant structural change.) Additional support for the inflexibility of the macrocycles **5** and **6** comes from the X-ray absorption observations that neither compound converts to a high-spin, hexacoordinate form on addition of piperidine whereas **1**–**3** do. F430 does convert to a high-spin form with significant changes (~0.2 Å) in the Ni(II)–N distances,[7,22] and thus F430 is quite flexible. (The Ni–N distances are comparable for the low-spin forms of F430, **5** and **6**, and therefore their affinity for axial ligands is expected to be roughly similar.[4d]) The structural compliance of the F430 skeleton has been attributed to its unique two *adjacent* meso methylenes, on the basis of molecular mechanics calculations,[58] features not present in **5** and **6**.

Conformational factors may also be relevant to reports that Ni(I) porphyrins can be generated in *N,N'*-dimethylformamide.[12,16] Kadish and co-workers have suggested[16] that reduction of *pentacoordinate* Ni(II), with the Ni out of plane, leads to Ni(I). Extended Hückel calculations for tetraaza complexes[20] and INDO computations[59] for porphyrins support this idea. Thus, here again, the ability of the Ni complexes to accommodate Ni–N changes appear to control the sites of reduction.

## Concluding Remarks

We have examined the reductive chemistry of a series of progressively more saturated Ni(II) porphyrin derivatives in order to gain some insights into the electronic and structural factors that control the chemistry of F430. Incorporation of the exocyclic cyclohexanone ring, also found in F430, has no obvious structural consequences but renders the macrocycles easier to reduce and harder to oxidize. Increased saturation of the compounds causes shifts in optical and redox properties, induces structural changes, and affects axial ligation and sites of reduction. With the exception of the isobacteriochlorins, the compounds are reduced to $\pi$ anion radicals or $\pi$ anion radicals with some degree of metal character. Only the isobacteriochlorins unambiguously yield Ni(I) as established by optical, EPR, and X-ray absorption results. Formation of Ni(I) leaves the metal tetracoordinate but induces a distortion in the Ni–N environment. The reason for the distortion is not obvious, but it may be an enhanced manifestation of the differences in M–N distances often observed in hydroporphyrins in which the M–N bonds to the saturated pyrroline rings are longer than those to the pyrroles.[49–51] A similar asymmetry is found in the X-ray structure of a Cu(II) isobacteriochlorin, another $d^9$ configuration.[60] In contrast, formation of $\pi$ anion radicals has little effect on the macrocycle, not surprisingly, since the added electron is distributed over the entire molecule rather than being localized in the metal $d_{x^2-y^2}$ orbital. The different sites of reduction lead to different reactivities. Ni(I) species react catalytically with methyl halides[6,8,9] whereas $\pi$ radicals are either inert or are attacked at the periphery,[16] again consonant with the localization or delocalization of the reducing electron.

In addition to the effects of saturation in determining energy levels and hence reactivities, structural effects emerge as significant factors in controlling the properties of the Ni compounds. In order to form Ni(I) or hexacoordinate high-spin Ni(II), the compounds must be flexible enough to accommodate the conformational changes that accompany reduction to Ni(I) or axial ligation of square-planar Ni(II). Thus, combinations of electronic and structural factors control the chemistry of the models considered here and, by extrapolation, that of F430 as well.

**Acknowledgment.** This work was supported by the Division of Chemical Sciences, U.S. Department of Energy, under Contract DE-AC02-76CH00016 at Brookhaven National Laboratory, and by National Science Foundation Grant CHE90-01381 at the University of California, Davis. X-ray absorption experiments were performed at beam line X-11A of the National Synchrotron Light Source at BNL. X-11A is supported by the Division of Materials Sciences, U.S. Department of Energy, under Contrast DE-FG05-89ER45384.

**Supplementary Material Available:** Tables of complete crystal data for **3** and final positional and thermal parameters for the non-hydrogen atoms of **3**, figures of X-ray absorption data ($k^3$ weighed raw data, Fourier transforms, isolated first-shell EXAFS, and nonlinear least-squares fits for **1**–**6** and **2** + 5 M piperidine (Figures 1–3S)), and an energy level diagram for **1**–**6** calculated by the extended Hückel method (Figure 4S) (13 pages); table of calculated and observed structure factors for **3** (7 pages). Ordering information is given on any current masthead page.

(57) Cullen, D. L.; Meyer, E. F. *J. Am. Chem. Soc.* **1974**, *96*, 2095.

(58) Zimmer, M.; Crabtree, R. M. *J. Am. Chem. Soc.* **1990**, *112*, 1062.

(59) Cory, M.; Zerner, M. C. Private communication. We have obtained similar results using IEH calculations.

(60) Chang, C. K.; Barkigia, K. M.; Hanson, L. K.; Fajer, J. *J. Am. Chem. Soc.* **1986**, *108*, 1342.